REVISTA ENERGIA NA AGRICULTURA

DOI: http://dx.doi.org/10.17224/EnergAgric.2017v32n1p65-71

ISSN: 1808-8759 (cd-rom)
2359-6562 (on-line)

A METHOD FOR CALCULATING THE SLOPE ERROR OF MIRRORED SURFACES CONSISTED OF FACETS CURVED IN ONE AXIS USED IN CONCENTRATED SOLAR POWER (CSP) TOWER SYSTEMS

Joachim Göttsche[1], Marcelo Lampkowski[2], Pedro Henrique Silva Bezerra[3], Érico Tadao Teramoto[4] & Cristiano Teixeira Boura[5]

ABSTRACT: Heliostats are considered the most important cost elements of a Concentrated Solar Power (CSP) power tower system and the use of suitable heliostats can generate reductions up to 40% in the power losses. Therefore, the design and optimization of heliostats have a great importance in solar tower power plant projects. This technical brief aims to present a method for calculating the slope error of bended-mirrored surfaces used in CSP power tower systems. For that, a heliostat composed by six mirror facets measuring 2.5 meters (width) x 0.533 meters (height) each, curved only in one axis and with a 30 meters' focal length was considered. The found slope errors results using the numerical approach and the analytical approach were very similar, suggesting that both methods are applicable in this case.

KEYWORDS: Heliothermic, heliostat, renewable energy, solar thermal power.

UM MÉTODO PARA CÁLCULO DO ERROR DE INOPERAÇÃO DE SUPERFÍCIES MIRRORADAS CONSIDERADAS DE FACETES CURVIDAS EM UM EIXO USADO EM SISTEMAS DE TORRE DE FORNECIMENTO SOLAR CONCENTRADO (CSP)

RESUMO: Os heliostatos são considerados os elementos mais importantes em relação ao custo de uma usina de energia solar concentrada (CSP) baseada em tecnologia de torre central e o uso de heliostatos adequados pode gerar reduções de até 40% nas perdas de energia. Portanto, o design e otimização de heliostatos tem grande importância nos projetos de plantas deste tipo. Este trabalho visa apresentar um método para calcular o erro de deformação das superfícies espelhadas curvadas utilizadas nos sistemas CSP de torre de energia. Para isso, foi considerado um heliostato composto por seis facetas espelhadas de 2,5 metros (largura) x 0,533 metros (altura) cada, curvadas apenas em um eixo e com uma distância focal de 30 metros. Os resultados encontrados nos erros de deformação usando a abordagem numérica e a abordagem analítica foram muito semelhantes, sugerindo que ambos os métodos são aplicáveis neste caso.

1 INTRODUCTION

Concentrating Solar Power (CSP) technology is poised to take its place as one of the major contributors to the future clean energy matrix. CSP does not pollute during its use, it comes from a renewable resource and it is increasingly becoming an economically viable. CSP technology is based on the use of mirrored surfaces that reflects and concentrates the direct solar irradiation in order to convert it into thermal energy, from which it generates water vapor that will trigger a reversible thermodynamic cycle that converts heat into work, known as Rankine.

CSP technologies involve the following phases: collection and concentrating of solar radiation; absorption of the radiation in a receiver as thermal energy; transporting the thermal energy to the power conversion system; converting thermal energy into electrical energy (EPE, 2012). In summary, CSP plants concentrate beams of light from the sun to heat a fluid and produce steam. The steam rotates a turbine connected to a generator, producing electricity to run a traditional power plant (CORGOZINHO; MARTINS NETO; CORGOZINHO, 2014).

The main settings of CSP plants are the cylindrical-parabolic troughs concentrators; linear Fresnel concentrators, parabolic dish concentrators (also known as dish/engine systems); and heliostats arrangements, redirecting sunlight to a stationary receiver (power tower) (SILVA, 2013). The first type uses mirrors in the form of parabolic troughs absorber disposed at the focal line of the collector, generally consisting of a metal tube

[1e 5] Solar-Institut Jülich . Email: goettsche@sij.fh-aachen.de ; boura@sij.fh-aachen.de
[2e 3] FCA/UNESP Botucatu. Emails: marcelo-l@uol.com.br ; bezerra_ph@hotmail.com
[4] Unesp- Campus de Registro. Email: ericoengineer@fca.unesp.br

coated with a layer of selective paint and wrapped for a second glass tube whose space between they should be evacuated to avoid losses by convection. The second type, based on Fresnel technology, uses mobile linear reflectors to concentrate the radiation on fixed linear absorber. The third type consists of parabolic dishes, which are reflectors of paraboloid shape, in most cases, with a group motor / generator for each individual reflector located at the focal point. Finally, the fourth type of technology is called solar tower, in which use thousands of mirrors to concentrate the sunlight on a fixed central tower (CORGOZINHO; MARTINS NETO; CORGOZINHO, 2014). All four types of CSP technology uses sun tracking to increase funding and ensure that the rays are reflected at the point of interest.

CSP plants based on central tower consists in a field of heliostats (devices that tracks the sun's movement and usually use a mirror or set of mirrors that can be targeted throughout the day through a fixed axis to redirect sunlight into a stationary receiver) that moves independently, and a concentrator located at the top of a tower. Each heliostat moves to reflect the sun's rays to the concentrator. The concentrator consists of a tube in which circulates a thermal fluid that is heated by the reflected sunlight (EPE, 2012).

According to Silva (2013), on a solar tower system, heliostats (mirror surfaces that follow the sun) act as solar collectors, concentrating solar radiation on a central receiver located on top of the tower. The central tower is a heat exchanger (receiver), where the energy is transferred to a heat a thermal fluid. This is optionally stored and finally passed to a system for converting thermal energy into electrical energy by the steam cycle, as can be seen in Figure 1.

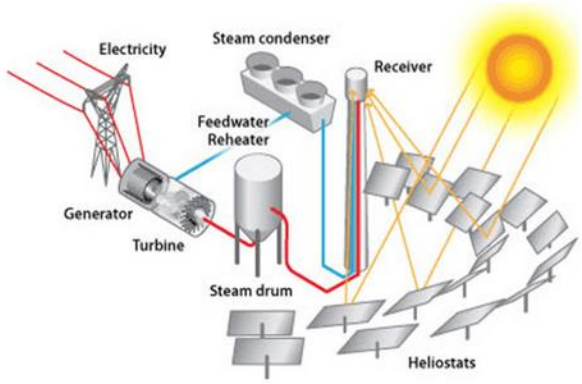

Figure 1 – *Operating diagram of a CSP power tower system.*
Source*: U.S. Department of Energy - Energy Efficiency & Renewable Energy.*

A heliostat is a device that includes a mirror or a set of mirrors, plane or bended, which turns so as to keep reflecting sunlight toward a predetermined target, compensating for the sun's apparent motions in the sky. The target usually is located distant from the heliostat and, in almost every case, it is stationary relative to the heliostat, so the light is reflected in a fixed direction. Heliostats are considered the most important cost elements of power tower CSP system. They can represent between 40 and 50% of the initial investment (KOLB et al., 2014). Furthermore, the use of suitable heliostats can generate reductions up to 40% in the power loses (KOLB et al., 2007).

Based on the considerations above and also in papers developed by Kolb et al. (2014), Landman and Gauché (2014); and Larmuth, Malan and Gauché (2014), that also highlight the importance of the design and analysis of the performance of heliostats to power tower CSP projects, the main objective of this technical brief is to present a method for calculating the slope error of one axis bended-mirrored surfaces used in Concentrated Solar Power (CSP) tower systems. The slope error results from deviations of the mirror curvature from the ideal shape and imperfections of the reflecting surface due to waviness and roughness lead to deflections of the reflected ray from the intended direction. It is the area weighted local misalignment compared with an ideal parabolic shape.

The perspective of contribution of this brief is based on the efficient application of CSP-based technologies and also on the encouragement of use of alternative renewable sources to generate electricity and heat. CSP technology has great potential to appliance in any area involving commercial or non-commercial purposes.

2 MATERIAL AND METHODS

To calculate the slope error, it was considered a set of six (6) mirror facets measuring 2.5 meters (width) x 0,533 meters (height); one mirror in a row by six in a single column, as can be seen in Figure 2. In order to minimize the tension in the glass, the facets are only curved in one axis.

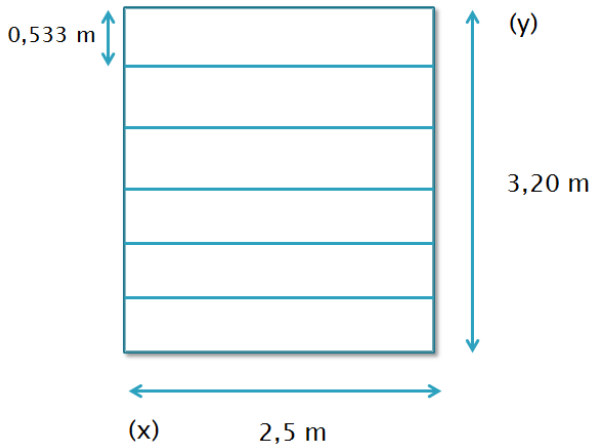

Figure 2 – *Heliostat composed by six mirror facets measuring 2.5 meters (width) x 0,533 meters (height) each.*
Source*: Developed by the authors.*

In addition, it was considered that the heliostat has a 30-

meter focal length. The focal length is the distance between the mirror middle and the smallest focal spot that the reflected beam can produce. This influences the mirror curvature (bending).

The original idea was to use a single mirror with 2.5 meters (width) x 3,20 meters (height), but computer simulations made using SOLCAL, a ray tracer software developed at the Solar-Institut Jülich, indicated that using the six stripes facets heliostat results in about 20% improvement on energy losses through spillage if compared to the single facet heliostat.

Two types of approaches were used: a numerical one and an analytical one. Of the steps that will be presented next, the first four are directly related to the numerical method. Step number five refers to the analytical approach that will be used to compare the final results.

1. Definition of the normal vector. In three-dimensional (3D) domain, the normal vector is the one that makes 90 degrees; perpendicular to a given surface to which it refers.

2. Considering that the slope error results from deviations of the mirror curvature from the ideal shape, the next step was related to find the results of an ideal parabola (shape).

For the steps 1 and 2, the following equations were used in this study:

Ideal parabola:

$$z = \frac{x^2 + y^2}{4f} \quad (1)$$

Another representation of the same surface is:

$$F(x,y,z) = -\frac{x^2+y^2}{4f} + z \text{ , with:} \quad (2)$$

$$F(x,y,z) = 0.$$

The normal vector to that surface $\underset{n}{\rightarrow}$ is defined as:

$$\underset{n}{\rightarrow} = \begin{pmatrix} \frac{\partial F}{\partial x} \\ \frac{\partial F}{\partial y} \\ \frac{\partial F}{\partial z} \end{pmatrix} \text{ , with:} \quad (3)$$

$$\frac{\partial F}{\partial x} = -\frac{\partial z}{\partial x} = -\frac{x}{2f}$$

$$\frac{\partial F}{\partial y} = -\frac{\partial z}{\partial y} = -\frac{y}{2f}$$

$$\frac{\partial F}{\partial z} = 1.$$

The unit normal vector $\underset{u}{\rightarrow}$ is given by:

$$\underset{u}{\rightarrow} = \frac{\vec{n}}{\sqrt{1 + \frac{x^2+y^2}{4f^2}}} \quad (4)$$

3. The next step was to find the constant slope of the facets (of width b) in the y axis. For that, the equations used are shown:

$$\text{If } 0 \le y < b, \text{ then: } F(x,y,z) = \frac{x^2}{4f} + c1 * y - z \quad (5)$$

$$\text{If } b \le y < 2b, \text{ then: } F(x,y,z) = \frac{x^2}{4f} + c2 * y - z \quad (6)$$

$$\frac{\partial F}{\partial x} = -\frac{x}{2f} \quad (7)$$

$$\frac{\partial F}{\partial y} = c1, c2, \ldots \quad (8)$$

$$c1 = \frac{\frac{b}{2}}{2f} = \frac{b}{4f} \quad (9)$$

$$c2 = \frac{\frac{3b}{2}}{2f} = \frac{3b}{4f} \quad (10)$$

A general formula of the slope along the y axis at any point (x, y) on the mirror for any stripe width *b* can be derived:

$$c(y) = \left(\text{int}\left(\frac{y}{b} + \frac{1}{2}\right) - \frac{1}{2}\right) * \frac{b}{(2f)} \quad (11)$$

being independent of x.

4. Then, it was necessary to find the difference between the ideal parabola (shape) $\underset{u\_ideal}{\longrightarrow}$ and the shape considering the stripes approach $\underset{u\_stripes}{\longrightarrow}$ at each point (x, y) on the mirror surface. The slope error was calculated as follows:

$$slope\ error(x,y) = \left| \underset{u_{ideal}}{\longrightarrow}(x,y) - \underset{u_{\text{stripes}}}{\longrightarrow}(x,y) \right| \quad (12)$$

5. The initial four steps are related to the numerical approach of calculating the surface slope error. Finally, an analytical approach can be used just to compare the final results. In Figure 3, the slope in y direction is presented as a function of y for the ideal case (parabola) as linearly increasing, and the "stripes" approach as being a step wise function.

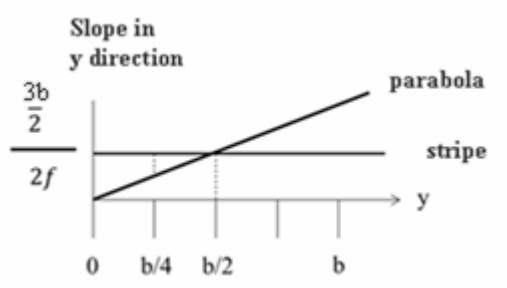

Figure 3 – *Graphical representation of the average slope, considering the parabola and the stripes approach.*

Given the graphical representation above (Figure 3) and the linearity of the problem, it can be concluded that the average slope error can be calculated by:

$$\text{Average slope error} = ½ * \frac{(b/2)}{(2f)} = \frac{b}{8f} \quad \ldots\ldots\ldots\ldots (13)$$

As the facet shape in x direction corresponds to the ideal parabolic shape, this can be considered as the overall slope error introduced by the "stripes" facet approach. In this particular case (b = 0.533 m, f = 30m), the error is e = 2.22 mrad. This appears to be acceptable although it must be considered that in practice, additional errors will result from the unevenness of the mirror surface, especially depending on the way in which the mirror facets are mounted at the heliostat frame.

3 RESULTS AND DISCUSSION

First, the ideal parabola was designed and the results for the X axis are shown on Table 1, using a 5 cm mirror interval and that the mirror has 2.5 m width.

Table 1 – *Mirror deviation representation in X axis, considering the ideal parabola (mirror: 2.5 m x 3.20 m).*

Mirror width (m)	Deviation (rad)
-1,25	0,021
-1,2	0,020
-1,15	0,019
-1,1	0,018
-1,05	0,017
-1	0,017
-0,95	0,016
-0,9	0,015
-0,85	0,014
-0,8	0,013
-0,75	0,012
-0,7	0,012
-0,65	0,011
-0,6	0,010
-0,55	0,009
-0,5	0,008
-0,45	0,007
-0,4	0,007
-0,35	0,006
-0,3	0,005
-0,25	0,004
-0,2	0,003
-0,15	0,002
-0,1	0,002
-0,05	0,001
0	0
0,05	-0,001
0,1	-0,002
0,15	-0,002
0,2	-0,003
0,25	-0,004
0,3	-0,005
0,35	-0,006
0,4	-0,007
0,45	-0,007
0,5	-0,008
0,55	-0,009
0,6	-0,010
0,65	-0,011
0,7	-0,012
0,75	-0,012
0,8	-0,013
0,85	-0,014
0,9	-0,015
0,95	-0,016
1	-0,017
1,05	-0,017
1,1	-0,018
1,15	-0,019
1,2	-0,02
1,25	-0,021

The results for the ideal parabola related to the Y axis can be seen on Table 2, considering a 5 cm mirror interval and that the mirror has 3.2 m height. The X axis only shows the first three 5 cm intervals; the results are the same for the whole X axis.

Table 2 – *Mirror deviation representation in Y axis, considering the ideal parabola (mirror: 2.5 m x 3.20 m).*

Mirror (Y) (m)	Mirror (X) (m)			
	-1,25	-1,2	-1,15	-1,1
	Deviation (rad)			
1,6	-0,027	-0,027	-0,027	…
1,55	-0,026	-0,026	-0,026	…
1,5	-0,025	-0,025	-0,025	…
1,45	-0,024	-0,024	-0,024	…
1,4	-0,023	-0,023	-0,023	…
1,35	-0,022	-0,022	-0,022	…
1,3	-0,022	-0,022	-0,022	…
1,25	-0,021	-0,021	-0,021	…
1,2	-0,020	-0,020	-0,020	…
1,15	-0,019	-0,019	-0,019	…
1,1	-0,018	-0,018	-0,018	…
1,05	-0,017	-0,017	-0,017	…
1	-0,017	-0,017	-0,017	…
0,95	-0,016	-0,016	-0,016	…
0,9	-0,015	-0,015	-0,015	…
0,85	-0,014	-0,014	-0,014	…
0,8	-0,013	-0,013	-0,013	…
0,75	-0,012	-0,012	-0,012	…
0,7	-0,012	-0,012	-0,012	…

0,65	-0,011	-0,011	-0,011	…
0,6	-0,010	-0,010	-0,010	…
0,55	-0,009	-0,009	-0,009	…
0,5	-0,008	-0,008	-0,008	…
0,45	-0,007	-0,007	-0,007	…
0,4	-0,007	-0,007	-0,007	…
0,35	-0,006	-0,006	-0,006	…
0,3	-0,005	-0,005	-0,005	…
0,25	-0,004	-0,004	-0,004	…
0,2	-0,003	-0,003	-0,003	…
0,15	-0,002	-0,002	-0,002	…
0,1	-0,002	-0,002	-0,002	…
0,05	-0,001	-0,001	-0,001	…
0	0,000	0,000	0,000	…
-0,05	0,001	0,001	0,001	…
-0,1	0,002	0,002	0,002	…
-0,15	0,002	0,002	0,002	…
-0,2	0,003	0,003	0,003	…
-0,25	0,004	0,004	0,004	…
-0,3	0,005	0,005	0,005	…
-0,35	0,006	0,006	0,006	…
-0,4	0,007	0,007	0,007	…
-0,45	0,007	0,007	0,007	…
-0,5	0,008	0,008	0,008	…
-0,55	0,009	0,009	0,009	…
-0,6	0,010	0,010	0,010	…
-0,65	0,011	0,011	0,011	…
-0,7	0,012	0,012	0,012	…
-0,75	0,012	0,012	0,012	…
-0,8	0,013	0,013	0,013	…
-0,85	0,014	0,014	0,014	…
-0,9	0,015	0,015	0,015	…
-0,95	0,016	0,016	0,016	…
-1	0,017	0,017	0,017	…
-1,05	0,017	0,017	0,017	…
-1,1	0,018	0,018	0,018	…
-1,15	0,019	0,019	0,019	…
-1,2	0,020	0,020	0,020	…
-1,25	0,021	0,021	0,021	…
-1,3	0,022	0,022	0,022	…
-1,35	0,022	0,022	0,022	…
-1,4	0,023	0,023	0,023	…
-1,45	0,024	0,024	0,024	…
-1,5	0,025	0,025	0,025	…
-1,55	0,026	0,026	0,026	…
-1,6	0,027	0,027	0,027	…

For the z axis, the deviation values were always 1.

After the values related to the ideal parabola were discovered, the six stripes measuring 0.533 m width were considered and the deviations of x; y and z axis were calculated. For the X axis, results were practically the same as the ideal parabola. Deviations on the X axis from the perfect parabola in comparison to the stripes approach only started to appear when five or more decimal places were set.

Table 3 presents the values of the mirror deviation on the Y axis of the six stripes approach. The X axis only shows the first three 5 cm intervals; the results are the same for the whole X axis.

Table 3 – *Mirror deviation representation in Y axis, considering a heliostat composed by six mirror facets (2.5 m x 0.533 m each).*

Mirror (Y) (m)	Mirror (X) (m)				
	-1,25	-1,2	-1,15	-1,1	
	Deviation (rad)				
1,6	-0,022	-0,022	-0,022	…	STRIPE #1
1,55	-0,022	-0,022	-0,022	…	
1,5	-0,022	-0,022	-0,022	…	
1,45	-0,022	-0,022	-0,022	…	
1,4	-0,022	-0,022	-0,022	…	
1,35	-0,022	-0,022	-0,022	…	
1,3	-0,022	-0,022	-0,022	…	
1,25	-0,022	-0,022	-0,022	…	
1,2	-0,022	-0,022	-0,022	…	
1,15	-0,022	-0,022	-0,022	…	
1,1	-0,022	-0,022	-0,022	…	
1,05	-0,013	-0,013	-0,013	…	STRIPE #2
1	-0,013	-0,013	-0,013	…	
0,95	-0,013	-0,013	-0,013	…	
0,9	-0,013	-0,013	-0,013	…	
0,85	-0,013	-0,013	-0,013	…	
0,8	-0,013	-0,013	-0,013	…	
0,75	-0,013	-0,013	-0,013	…	
0,7	-0,013	-0,013	-0,013	…	
0,65	-0,013	-0,013	-0,013	…	
0,6	-0,013	-0,013	-0,013	…	
0,55	-0,013	-0,013	-0,013	…	
0,5	-0,004	-0,004	-0,004	…	STRIPE #3
0,45	-0,004	-0,004	-0,004	…	
0,4	-0,004	-0,004	-0,004	…	
0,35	-0,004	-0,004	-0,004	…	
0,3	-0,004	-0,004	-0,004	…	
0,25	-0,004	-0,004	-0,004	…	
0,2	-0,004	-0,004	-0,004	…	
0,15	-0,004	-0,004	-0,004	…	
0,1	-0,004	-0,004	-0,004	…	
0,05	-0,004	-0,004	-0,004	…	
0	-0,004	-0,004	-0,004	…	
-0,05	0,004	0,004	0,004	…	STRIPE #4
-0,1	0,004	0,004	0,004	…	
-0,15	0,004	0,004	0,004	…	
-0,2	0,004	0,004	0,004	…	
-0,25	0,004	0,004	0,004	…	
-0,3	0,004	0,004	0,004	…	
-0,35	0,004	0,004	0,004	…	
-0,4	0,004	0,004	0,004	…	
-0,45	0,004	0,004	0,004	…	
-0,5	0,004	0,004	0,004	…	
-0,55	0,013	0,013	0,013	…	STRIPE #5
-0,6	0,013	0,013	0,013	…	
-0,65	0,013	0,013	0,013	…	
-0,7	0,013	0,013	0,013	…	
-0,75	0,013	0,013	0,013	…	
-0,8	0,013	0,013	0,013	…	
-0,85	0,013	0,013	0,013	…	
-0,9	0,013	0,013	0,013	…	
-0,95	0,013	0,013	0,013	…	
-1	0,013	0,013	0,013	…	
-1,05	0,013	0,013	0,013	…	
-1,1	0,022	0,022	0,022	…	STRIPE #6
-1,15	0,022	0,022	0,022	…	
-1,2	0,022	0,022	0,022	…	
-1,25	0,022	0,022	0,022	…	
-1,3	0,022	0,022	0,022	…	

-1,35	0,022	0,022	0,022	…	
-1,4	0,022	0,022	0,022	…	
-1,45	0,022	0,022	0,022	…	
-1,5	0,022	0,022	0,022	…	
-1,55	0,022	0,022	0,022	…	
-1,6	0,022	0,022	0,022	…	

As it happened for the ideal parabola, for the z axis, the deviation values were always 1, also in the stripes approach.

Finally, the difference between the x; y and z axis were calculated. For that, the following equation was built in Microsoft Excel and a graphical representation of the values is shown on Table 4.

$$\sqrt{(Xs - Xid)^2 + (Ys - Yid)^2 + (Zs - Zid)^2} \quad (14)$$

Being,

- Xs, X axis stripes approach;
- Xid, X axis ideal parabola;
- Ys, Y axis stripes approach;
- Yid, Y axis ideal parabola;
- Zs, Z axis stripes approach;
- Zid, Z axis ideal parabola;

Table 4 – *Difference between the x; y and z axis comparing the stripes approach and the ideal parabola.*

Mirror (Y) (m)	Mirror (X) (m)			
	-1,25	-1,2	-1,15	-1,1
	Deviation (rad)			
1,6	0,0044	0,0044	0,0044	…
1,55	0,0036	0,0036	0,0036	…
1,5	0,0028	0,0028	0,0028	…
1,45	0,0019	0,0019	0,0019	…
1,4	0,0011	0,0011	0,0011	…
1,35	0,0003	0,0003	0,0003	…
1,3	0,0006	0,0006	0,0006	…
1,25	0,0014	0,0014	0,0014	…
1,2	0,0022	0,0022	0,0022	…
1,15	0,0031	0,0031	0,0031	…
1,1	0,0039	0,0039	0,0039	…
1,05	0,0042	0,0042	0,0042	…
1	0,0033	0,0033	0,0033	…
0,95	0,0025	0,0025	0,0025	…
0,9	0,0017	0,0017	0,0017	…
0,85	0,0008	0,0008	0,0008	…
0,8	0,0000	0,0000	0,0000	…
0,75	0,0008	0,0008	0,0008	…
0,7	0,0017	0,0017	0,0017	…
0,65	0,0025	0,0025	0,0025	…
0,6	0,0033	0,0033	0,0033	…
0,55	0,0042	0,0042	0,0042	…
0,5	0,0039	0,0039	0,0039	…
0,45	0,0031	0,0031	0,0031	…
0,4	0,0022	0,0022	0,0022	…
0,35	0,0014	0,0014	0,0014	…
0,3	0,0006	0,0006	0,0006	…
0,25	0,0003	0,0003	0,0003	…
0,2	0,0011	0,0011	0,0011	…
0,15	0,0019	0,0019	0,0019	…
0,1	0,0028	0,0028	0,0028	…
0,05	0,0036	0,0036	0,0036	…
0	0,0044	0,0044	0,0044	…
-0,05	0,0036	0,0036	0,0036	…
-0,1	0,0028	0,0028	0,0028	…
-0,15	0,0019	0,0019	0,0019	…
-0,2	0,0011	0,0011	0,0011	…
-0,25	0,0003	0,0003	0,0003	…
-0,3	0,0006	0,0006	0,0006	…
-0,35	0,0014	0,0014	0,0014	…
-0,4	0,0022	0,0022	0,0022	…
-0,45	0,0031	0,0031	0,0031	…
-0,5	0,0039	0,0039	0,0039	…
-0,55	0,0042	0,0042	0,0042	…
-0,6	0,0033	0,0033	0,0033	…
-0,65	0,0025	0,0025	0,0025	…
-0,7	0,0017	0,0017	0,0017	…
-0,75	0,0008	0,0008	0,0008	…
-0,8	0,0000	0,0000	0,0000	…
-0,85	0,0008	0,0008	0,0008	…
-0,9	0,0017	0,0017	0,0017	…
-0,95	0,0025	0,0025	0,0025	…
-1	0,0033	0,0033	0,0033	…
-1,05	0,0042	0,0042	0,0042	…
-1,1	0,0039	0,0039	0,0039	…
-1,15	0,0031	0,0031	0,0031	…
-1,2	0,0022	0,0022	0,0022	…
-1,25	0,0014	0,0014	0,0014	…
-1,3	0,0006	0,0006	0,0006	…
-1,35	0,0003	0,0003	0,0003	…
-1,4	0,0011	0,0011	0,0011	…
-1,45	0,0019	0,0019	0,0019	…
-1,5	0,0028	0,0028	0,0028	…
-1,55	0,0036	0,0036	0,0036	…
-1,6	0,0044	0,0044	0,0044	…

The average of the whole difference sheet was calculated and the slope error result was 2.256 mrad.

Finally, the analytical approach was used compare the final results on the numerical approach.

Considering the average slope error equals b/8f, the found result was 2.222 mrad. As seen, the final results for the mirror stripes were very close.

4 CONCLUSIONS

The slope error result using the numerical approach was 2.256 mrad and 2.22 mrad when the analytical method was used. The closeness of the results and the application of different numbers of facets with different height measurements demonstrated and proved that both approaches can be applied in this case. As the angular shape of the sun is ± 4.6 mrad, it was decided that the slope error of 2.2 mrad could be acceptable, and a heliostat mirror with 6 stripes could be a reasonable compromise between low cost and high optical quality.

5 ACKNOWLEDGEMENTS

This technical brief is part of the final results related to the i-NoPa/CIESA project, titled “Studies of

heliothermic (solar thermal) energy (CSP – Concentrated Solar Power): consortium for educational integration and sustainability of agro-industry". I-NoPa/CEISA project is an initiative of academic cooperation between Brazil and Germany and the partnership involves the following institutions: Coordenação de Aperfeiçoamento de Pessoal de Nível Superior (CAPES); Deutscher Akademischer Austausch Dienst (DAAD) and Deutsche Gesellschaft für Internationale Zusammenarbeit (GIZ). The authors would like to thanks the mentioned institutions for their support.

6 REFERENCES

CORGOZINHO, I. M.; MARTINS NETO, J. H.; CORGOZINHO, A. **A. Modelo de simulação de uma planta solar-elétrica utilizando o software Trnsys**. V Congresso Brasileiro de Energia Solar. Recife, 31.04.2014.

EPE. **Análise da inserção da geração solar na matriz elétrica brasileira**. Nota técnica. Ministério de Minas e Energia. Rio de Janeiro, mai. 2012. Available at <http://pt.scribd.com/doc/213250230/NT-EnergiaSolar-2012>. Date of access: 29.05.2014.

KOLB, G. J.; JONES, S. A.; DONNELLY, M. W.; GORMAN, D.; THOMAS, R.; DAVENPORT, R.; LUMIA, R. **Heliostat cost reduction study**, SAND 2007: Available at <http://www.prod.sandia.gov/cgi-bin/techlib/access-control.pl/2007/073293.pdf>. Date of access: 15.09.2014.

KOLB, J. G.: JONES, S. A.; DONNELLY, M. W.; GORMAN, D.; THOMAS, R.; DAVENPORT, R.; LUMIA R. **Sandia report**: heliostat cost reduction study. California, USA, 2007. Available at <http://energy.sandia.gov/wp/wp-content/gallery/uploads/Heliostat_Cost_Reduction_SAND2007-3293.pdf>. Date of access: 15.09.2014.

LANDMAN, W.; GAUCHÉ, P. **Influence of canting mechanism and facet profile on heliostat field performance**. SolarPACES 2013. Energy Procedia, v. 49, 2014, p. 126–135.

LARMUTH, J.; MALAN, K. and GAUCHÉ, P. **Design and cost review of 2m² heliostat prototypes**. Proceedings of SASEC 2014. Port Elizabeth, South Africa, 2014.

SILVA, M. A. P. da. **Central de produção de energia eléctrica a partir de energia solar térmica**. Dissertação (Mestrado em Engenharia Mecânica)- Instituto Superior de Engenharia de Lisboa. Departamento de Engenharia Mecânica. Lisboa, 2013.